

Pattern Formation in the Transverse Section of a Laser with a Large Fresnel Number

S. P. Hegarty, G. Huyet,* and J. G. McInerney

Physics Department, National University of Ireland, University College, Cork, Ireland

K. D. Choquette

Photonics Research Department, Sandia National Laboratories, Albuquerque, New Mexico 87185

(Received 14 July 1998)

We experimentally investigate pattern formation in a single-wavelength long laser cavity with a large Fresnel number. Near the laser threshold, we observe a single frequency spatially periodic structure corresponding to tilted waves theoretically predicted by the Maxwell-Bloch equations. We also show the presence of secondary instabilities at other wavelengths and polarization instabilities at the same wavelength for different parameter values. [S0031-9007(99)08512-9]

PACS numbers: 42.65.Sf, 42.55.Px, 42.60.Mi

Pattern formation in dissipative systems has been the subject of much research during the past 20 years [1]. In optics [2], activity has centered on research into chaos in lasers [3] and instabilities in passive systems [4–8]. From a theoretical viewpoint, lasers with large Fresnel numbers were analyzed with partial differential equations derived from the Maxwell-Bloch equations [9–11]. All of these models predicted the formation of periodic structures such as traveling waves and of localized structures such as optical vortices [10] or spatial solitons [12]. These instabilities have been investigated experimentally in many optical systems such as sodium vapor [4], photorefractive crystals [5–7], and liquid crystal light valves [8]. In lasers, experiments carried out with gas lasers have shown evidence of spatiotemporal complexity [13–15] but remained purely qualitative since the patterns arising from the first instability, i.e., the laser threshold, differed from those predicted by the model. The mirror curvature, the small Fresnel number at threshold, and the presence of several longitudinal modes probably constituted the main reasons for the discrepancies between theoretical predictions and experimental observations.

Theoretical models used to describe lasers with a large Fresnel number are usually based on amplitude equations [9,10,16] derived from the Maxwell-Bloch equations for a two-level system. These models are generally reduced to two-dimensional partial differential equations assuming a single longitudinal mode laser with a very large transverse section. The detuning, $\delta = \omega_a - \omega_c$, between the atomic resonance ω_a and the cavity frequency ω_c appears to be the most important parameter for the pattern selected at the laser threshold. If $\delta > 0$ (positive detuning), the laser will select a traveling wave solution with a transverse wave vector k_\perp such that its frequency is at the atomic frequency. If $\delta < 0$ (negative detuning), the laser selects a uniform plane wave solution.

This simple theoretical prediction has not yet been observed experimentally, at least in the case of a laser [6], mainly because experiments tended to be carried out on laser cavities with curved mirrors, as is necessary to

obtain large Fresnel numbers in long cavities. In such a cavity, the mirrors break the translational symmetry and the observed patterns remain highly symmetric with respect to the cavity optical axis, in particular privileging Gaussian beams. In addition, the mode spacing of a laser with curved mirrors operating with a large Fresnel is generally of the same order of magnitude as the transverse mode spacing. The pattern selected at threshold is therefore more complicated to analyze.

In this Letter, we present the first experimental results of pattern formation in a single-wavelength long laser cavity with a large Fresnel number. We use vertical cavity surface emitting semiconductor lasers (VCSELs) of very large transverse section and short cavity length [17]. Near the lasing threshold, the laser emits a single frequency solution corresponding to an almost one dimensional standing wave of the laser intensity. The transverse wave number of this pattern can be controlled with the detuning, δ , as is predicted by two-level models. For higher pump levels and other detuning values, two instabilities may occur. The first instability is associated with the appearance of modes with smaller transverse wave numbers, while the second is associated with a polarization instability at the same wave number. In VCSELs, as the optical axis is orthogonal to the junction plane, the polarization constraint is weaker than in edge-emitting semiconductor lasers and gas lasers with Brewster windows. Polarization instabilities in VCSELs have been the subject of much research during the past few years [18–20].

The experiment was carried out with large aperture native oxide confined VCSELs emitting around 850 nm. A schematic representation of the laser structure is shown in Fig. 1. In these lasers, the quantum well gain medium is sandwiched between two distributed Bragg reflectors (DBRs) to give a single wavelength long cavity. This very short cavity ensures single longitudinal mode operation. In order to define which portion of the quantum well layers shall have carriers injected, it is necessary to insert dielectric apertures above and below the active layers. This was achieved by etching square mesas through the

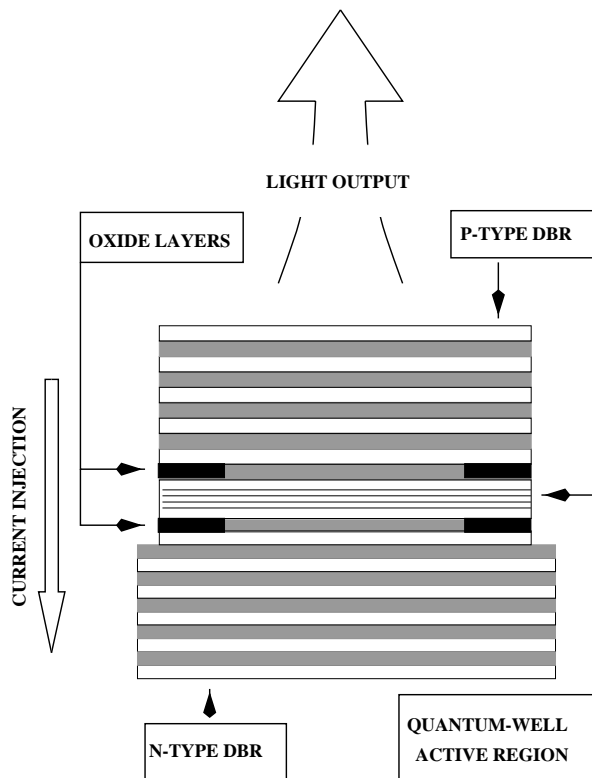


FIG. 1. Structure of a vertical cavity surface emitting laser with dielectric oxide confining layers.

active region and oxidising laterally a high Al content layer [21]. As the index of these oxide dielectric apertures is lower than that of the surrounding semiconductor, they also produced a transverse index difference and thus transverse optical confinement. The devices were electrically pumped with a low noise dc current source and mounted on a temperature controlled heat sink. The heat sink temperature and the injection current constituted the two experimental control parameters. The heat sink temperature controlled the detuning since it altered both the cavity resonance and the band gap energy (atomic frequency) but at markedly different rates [22]. For our lasers, the gain peak was in resonance with the fundamental mode of the cavity for a temperature of 25 °C. At lower temperatures, the gain peak frequency was higher than the cavity frequency. The injection current controlled the pump parameter though it had a secondary effect on the temperature of the active region, and thus the gain peak frequency, through the mechanism of Joule heating. The laser emission was either focused onto a CCD camera in order to analyze the near field, or scattered off a diffusion screen in the Fraunhofer limit to obtain the far field. Part of the light was also coupled to a fiber in order to study the optical spectrum and/or analyze the microwave spectrum of the laser intensity.

For small devices, less than $3 \times 3 \mu\text{m}^2$, the laser operated in its fundamental TEM_{00} mode. For side lengths between 3 and 15 μm , the lasers operated with several Gauss-Hermite/Laguerre transverse modes as observed in

Ref. [22]. In this article, we describe the behavior of larger lasers, with apertures between $15 \times 15 \mu\text{m}^2$ and $40 \times 40 \mu\text{m}^2$, where the dynamics differ from those previously observed. For these broad area VCSELs, the near field below threshold is almost spatially homogeneous (the fluctuations are smaller than 5%) indicating a nearly spatially uniform pump.

Just above the lasing threshold current, i_{th} , for low temperatures (below 25 °C), the near field consisted of an almost regular spatial modulation of the laser intensity as shown in Fig. 2 (top). The associated far field [Fig. 2 (bottom)] is centrally symmetric through the optical axis and concentrated on a highly divergent cone. Measurements of the optical spectrum showed that the laser was operating at a single frequency (side mode suppression ratio ~ 10 dB) and the light was polarized parallel to the stripes observed in the near field. As the power is divided equally between both tilted waves, the coherent emission forms a perfect standing wave in the near field. However, as we are operating close to threshold, the spontaneous power and stimulated power are comparable, and we get a modulation of around 50%. The transverse component in

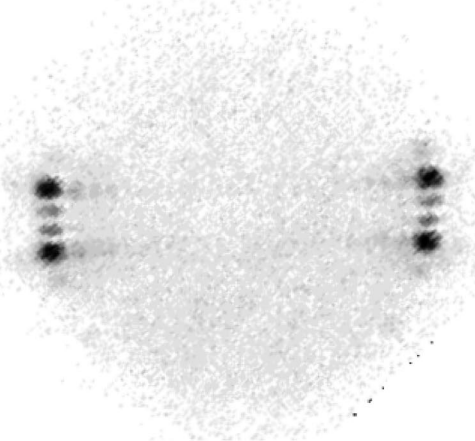
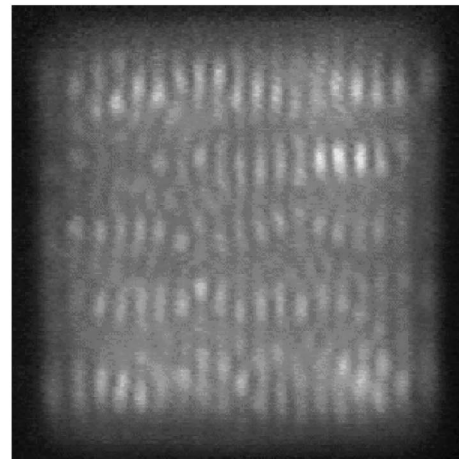


FIG. 2. Near field (top) and far field (bottom) of a single frequency standing wave of the laser intensity. The laser aperture is $15 \times 15 \mu\text{m}^2$. The spatial wavelength of the intensity of this pattern is approximately $0.75 \mu\text{m}$ and the corresponding divergence in air is 65° full angle.

the wave vector could be decreased by decreasing the detuning (increasing the temperature) as expected from the two-level model. The reduction in the transverse wave vector resulted in fewer stripes in the near field, this effect occurring in discrete steps rather than continuously. The symmetry of the far field and the modulation of the near field indicate a transverse standing wave of the electric field in the laser cavity. The theoretical prediction of the two-level model is for a standing wave solution to be unstable with respect to the traveling wave solution, which has an unmodulated near field (when averaged over long times). However, this prediction is made for an infinite system, whereas our system has a finite size [14,23]. Theoretical analysis of the Maxwell-Bloch equations with finite size have predicted standing waves near the solitary laser threshold. In our case, the current guiding oxide layers show a large index discontinuity with the surrounding semiconductor material. At large angles of incidence, a ray incident upon such an oxide boundary would undergo total internal reflection, generating a transverse standing wave. We constructed a Mach-Zehnder interferometer in order to investigate the spatial correlation of the structure. By overlapping different parts of the pattern, we observed interference fringes across the entire structure. This indicates that the observed structure is a coherent Fourier mode.

In order to investigate systematically the dependence of the broad area laser frequency upon the detuning, a VCSEL wafer was obtained with the cavity resonance

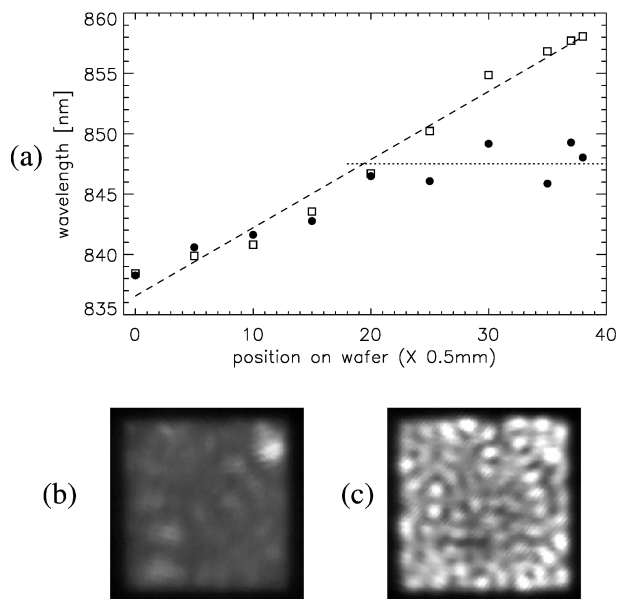


FIG. 3. (a) Laser wavelength as a function of position for both small and large VCSELs. Squares correspond to small Fresnel number lasers and dots to large Fresnel number lasers. The dashed line is a fit to the nearly linear variation of cavity resonance wavelength, the dotted line a fit to the broad area laser wavelength. (b) Near field of negatively detuned laser close to threshold. (c) Near field of negatively detuned laser at twice threshold.

varying as a function of position on the wafer. With this design, we could study lasers with different resonance frequencies but the same gain peak frequency. At each wafer position, both small ($3 \times 3 \mu\text{m}^2$) and large ($20 \times 20 \mu\text{m}^2$) VCSELs were fabricated. The small lasers always operated in the fundamental mode, thus yielding the cavity resonance wavelength at each position on the wafer, after a small correction to account for the finite transverse wave vector of the Gaussian mode. For the broad area devices the lasing wavelength at $1.1i_{\text{th}}$ was also measured as a function of position. The results are plotted in Fig. 3. For higher cavity frequency ($\lambda \lesssim 847 \text{ nm}$), the broad area laser frequency tracked the cavity resonance. Once the cavity frequency became less than a critical frequency (corresponding to 847 nm) the laser frequency remained more or less constant, and its wave vector acquired whatever k_{\perp} necessary so that it lased at the gain peak frequency. For experimental reasons it was not possible to obtain k_{\perp} during this measurement, but an increase in the far-field divergence with increasing detuning was observed. This result is in agreement with the theoretical predictions from the Maxwell-Bloch equations for both positive and negative detuning. However, the Maxwell-Bloch equations predict a plane wave solution for negative values of the detuning whereas the experiment shows a complicated low divergence pattern (see Figs. 3b and 3c) with an optical spectra containing many frequencies.

The fact that plane waves are not observed for negative detuning is probably due to the boundary conditions. It is well known that borders alter the pattern selected in a nonvariational system since they generate spatial modulation of the phase [24]. In Maxwell Bloch equations, the same mechanism occurs for both positive and negative detunings [14]. For negative detuning this effect appears clearly since a spatially modulated pattern appears instead of a plane wave solution. However, this effect is difficult to observe for positive detuning since it modifies only the selected wave number.

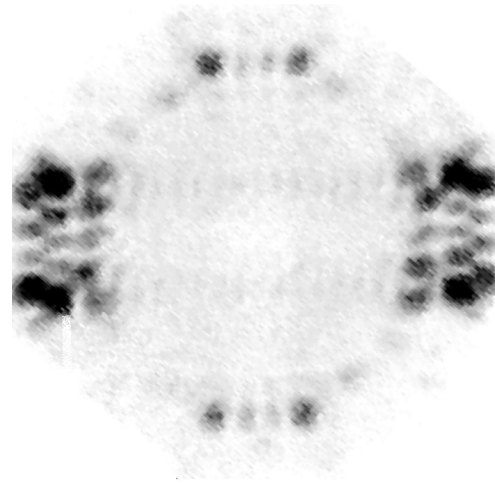


FIG. 4. Far field of the laser at 1.6 times lasing threshold, showing both the polarization and the multimode instabilities.

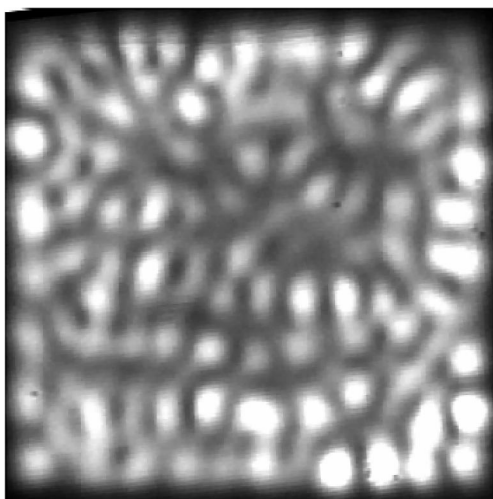


FIG. 5. Near field of the laser pumped at twice lasing threshold, containing many frequencies and polarizations. The laser is $25 \times 25 \mu\text{m}^2$.

When the temperature and/or the current were increased, two instabilities occurred. The first was associated with a polarization instability, when in addition to the pattern at threshold, there was superimposed on the near field a second pattern similar to the first after rotation through 90° . The wave vectors and polarization associated with the new pattern were also orthogonal to those of the original pattern. The second instability was associated with the onset of multimode operation. Initially one additional frequency appeared in the optical spectrum corresponding to emission in a lower transverse k vector in the far field. A far field displaying both instabilities is shown in Fig. 4. The near field remained highly ordered, but as the current was increased still further, other frequencies appeared and the optical spectrum became much broader, while the far field contained a full ring of low divergence k vectors. The time-averaged near-field lost order as is shown in Fig. 5.

In conclusion, we have experimentally investigated pattern formation in a single longitudinal mode laser with a large Fresnel number. For positive detuning close to threshold, we observed a single frequency spatially periodic structure in accordance with predictions of the Maxwell-Bloch equations. However, the boundary conditions still play an important role favoring standing wave solutions over the true traveling wave solutions predicted by the Maxwell-Bloch equations for infinite transverse domains. The boundary conditions are also important for negative detuning where the selected pattern can be described by several Gaussian modes. We also showed the presence of secondary instabilities at other wavelengths and polarization instabilities at the same wavelength for different parameter values.

We would like to thank for stimulating discussions, A. J. Kent, G. K. Harkness, W. J. Firth, and J. V. Moloney, for device fabrication H. Q. Hou, and for technical assistance and useful advice, R. Gillen, P. O'Brien, and K. M. Geib. One of us (G.H.) is supported by the Commission of the European Union. The work at Sandia National Laboratories was supported in part by the United States Department of Energy under Contract No. DE-AC04-94AL85000.

*Present address: Department of Physics and Applied Physics, University of Strathclyde, Glasgow, G4 ONG, Scotland, U.K.

- [1] M. C. Cross and P. C. Hohenberg, *Rev. Mod. Phys.* **65**, 851 (1993).
- [2] L. A. Lugiato *et al.*, in *Advances in Atomic, Molecular and Optical Physics*, edited by B. Bedersen and H. Walther (Academic Press, San Diego, 1999), Vol. 40, p. 229.
- [3] N. B. Abraham *et al.*, *Progress in Optics*, edited by E. Wolf (North-Holland, Amsterdam, 1988), Vol. XXV, p. 1.
- [4] T. Ackemann *et al.*, *Phys. Rev. Lett.* **75**, 3450 (1995).
- [5] F. T. Arecchi *et al.*, *Phys. Rev. Lett.* **67**, 3749 (1991).
- [6] A. V. Mamaev and M. Saffman, *Opt. Commun.* **128**, 281 (1996).
- [7] K. Staliunas *et al.*, *Phys. Rev. Lett.* **79**, 2658 (1997).
- [8] E. Pampaloni *et al.*, *Phys. Rev. Lett.* **74**, 258 (1995).
- [9] R. Lefever *et al.*, *Phys. Lett. A* **135**, 254 (1989).
- [10] P. Couillet *et al.*, *Opt. Commun.* **73**, 403 (1989).
- [11] G.-L. Oppo *et al.*, *Phys. Rev. A* **44**, 4712 (1991); G. D'Alessandro *et al.*, *Opt. Commun.* **131**, 172 (1996).
- [12] M. Brambilla *et al.*, *Phys. Rev. Lett.* **79**, 2042 (1997).
- [13] G. Huyet *et al.*, *Phys. Rev. Lett.* **75**, 4027 (1995); G. Huyet and J. R. Tredicce, *Physica (Amsterdam)* **96D**, 209 (1996); G. Huyet *et al.*, *Opt. Commun.* **127**, 257 (1996).
- [14] G. Huyet and S. Rica, *Physica (Amsterdam)* **96D**, 215 (1996).
- [15] E. Louvergnaux *et al.*, *Phys. Rev. A* **46**, 5955 (1992); D. Dangoisse *et al.*, *Phys. Rev. A* **53**, 4435 (1996).
- [16] J. Lega *et al.*, *Phys. Rev. Lett.* **73**, 2978 (1994); J. Lega *et al.*, *Physica (Amsterdam)* **83D**, 478 (1995).
- [17] W. W. Chow *et al.*, *J. Quant. Electron* **33**, 1810 (1997).
- [18] K. D. Choquette *et al.*, *Appl. Phys. Lett.* **64**, 2062 (1994).
- [19] J. Martin-Regalado *et al.*, *Opt. Lett.* **22**, 460 (1997).
- [20] M. P. van Exter, A. Al-Remawi, and J. P. Woerdman, *Phys. Rev. Lett.* **80**, 4875 (1998).
- [21] K. D. Choquette, K. L. Lear, R. P. Schneider, Jr., and K. M. Geib, *Appl. Phys. Lett.* **66**, 3413 (1995).
- [22] H. Li, T. L. Lucas, J. G. McInerney, and R. A. Morgan, *Chaos Solitons Fractals* **4**, 1619 (1994).
- [23] G. K. Harkness, W. J. Firth, J. B. Geddes, J. V. Moloney, and E. M. Wright, *Phys. Rev. A* **50**, 4310 (1994).
- [24] P. Couillet, T. Frisch, and F. Plaza, *Physica (Amsterdam)* **62D**, 75 (1993).